



Rainfall regime trends at annual and monthly scales in Catalonia (NE Spain) and indications of CO₂ emissions effects

Xavier Lana¹ · M. Carmen Casas-Castillo² · Raül Rodríguez-Solà¹ · Carina Serra¹ · M. Dolors Martínez³ · Ricard Kirchner²

Received: 12 May 2021 / Accepted: 6 September 2021 / Published online: 16 September 2021
© The Author(s) 2021, corrected publication 2022

Abstract

The pluviometric regime in the Western Mediterranean and concretely in Catalonia (NE Spain) is characterised by irregular amounts at monthly and annual scales, sometimes with copious short episodes causing floods and, conversely, sometimes with long dry spells exceeding 1 month length, depending on the chosen threshold level to define the dry episode. Taking advantage of a dense network of rain gauges, most of them with records length of 50–60 years and some others exceeding 85 years, the evolution of these monthly and annual amounts is quantified by means of their time trends, statistical significance and several irregularity parameters. In agreement with the evolution of the CO₂ emissions into the atmosphere and the increasing concentration, in parts per million (ppm), of this greenhouse gas, different time trends at annual scale have been detected up to approximately years 1960–1970 in comparison with the interval 1960–1970 to nowadays. Consequently, besides the greenhouse effects on the temperature regime, the influence on the pluviometric regime could not be negligible.

Keywords Western Mediterranean climate · Rainfall time trends · Pluviometric irregularity · CO₂ emissions effects

1 Introduction

The rainfall amounts at monthly and annual scale for Catalonia (NE Spain) are characterised by quite notable spatial and temporal irregularities. They are usually consequence of copious episodes of short length, sometimes causing flood events and usually associated with eastern advections or convective phenomena, the closeness to the Western Mediterranean playing a relevant role. Additionally, dry spells of notable length are also another characteristic of this pluviometric regime. Some examples of these complexities and irregularities, which include daily, monthly and annual amounts relationships with surface synoptic circulations,

annual extreme drought characteristics, and rainfall shortage characterised by the standardised precipitation index, SPI, have been analysed years ago by Serra et al. (1998), Lana and Burgueño (1998), Lana et al. (2001, 2004), Martínez et al. (2007) and Casas et al. (2007), among others.

Apart from all these characteristics of the rainfall pattern, negative time trends on rainfall amounts at monthly and annual scale would be another factor of complexity to design a right use of water resources for agriculture, industry, drinking water supply or generation of hydroelectric power, for instance. Flood episodes, caused by short intervals of copious rainfall amounts, contributing to the monthly rainfall irregularity, should be another question to be carefully analysed given that these episodes could affect metropolitan areas with high density of inhabitants (Lana et al. 2019, 2020b) or agricultural areas where harvests could be damaged.

Expected time trends on Western Mediterranean associated with the climatic change phenomenon (Pérez and Boscolo, 2010) and more concretely with an increment of CO₂ emissions (Meinshausen et al. 2017) are the main objective of this paper, distinguishing time trends for the complete recording rainfall and for the interval since 1960–1970 up to nowadays. Whereas the magnitude of every time trend

✉ M. Carmen Casas-Castillo
m.carmen.casas@upc.edu

¹ Department of Physics, ETSEIB, Universitat Politècnica de Catalunya-BarcelonaTech, Diagonal 647, 08028 Barcelona, Spain

² Department of Physics, ESEIAAT, Universitat Politècnica de Catalunya-BarcelonaTech, Colom 1, 08222 Terrassa, Spain

³ Department of Physics, ETSAB, Universitat Politècnica de Catalunya-BarcelonaTech, Diagonal 649, 08028 Barcelona, Spain

is quantified searching for a linear trend on every one of the series, the statistical significance of these time trends is determined by applying the Mann–Kendall test (Sneyers 1990). A possible relationship between annual CO₂ emissions and annual rainfall amounts is analysed by means of the cross-correlation between both types of annual data.

The contents of this paper are structured as follows. Section 1 (Database) describes the most relevant characteristics of the rain gauges network covering Catalonia (NE Spain), with a notable degree of data quality, which has been yet used in previous analyses. Section 2 details the most relevant climatic characteristics of the analysed area, including a brief description of the most relevant topographic features conditioning the different rainfall behaviours. Section 3 offers a complete and detailed description of the evolution detected on annual and monthly amounts, being possible to distinguish areas with positive and negative time trends and areas where these time trends achieve the highest statistical significance. Additionally, the evolution of the rainfall regime irregularity is analysed by means of several disparity indices and fractal theory. The evolution of annual amounts is compared in Section 4 with the corresponding CO₂ emissions, being quantified the degree of cross-correlation among both time series. The results obtained are summarised and discussed in Section 5, being qualitatively described the future expected characteristics of the pluviometric regime. Finally, the conclusions of this research are summarised in Section 6.

2 Database

The orography of Catalonia (NE Spain) is quite complex (Fig. 1a), with altitudes close to 2,900 m in some areas of the Eastern Pyrenees, 2,000 m in the Pre-Pyrenees, between 900 and 1,500 m in the Pre-Littoral chain, close to 500–600 m in the Central Basin and only a few hundred metres in the Littoral chain, contributing to its climatic diversity. Consequently, a dense pluviometric network is necessary. The 96 monthly and annual rainfall series have been obtained from *Servei Meteorològic de Catalunya* (SMC, www.meteo.cat), the meteorological agency of Catalonia, complemented with records from two other scientific organisations: Fabra Observatory (Reial Acadèmia de Ciències i Arts, RACA, Barcelona) and Ebro Observatory (Ramon Llull University, URL, and Consejo Superior de Investigaciones Científicas, CSIC, Spanish Government). The same dataset has been used (Lana et al. 2020a, 2021) to study several questions concerning rain amounts multifractal complexity and forecasting at monthly scale, with the aim of preventing forthcoming droughts episodes at monthly scale. Figure 1b details the distribution of the 96 rain gauges, which were chosen bearing in mind several constraints of data quality. First, tests of homogeneity and data quality (Llabrés-Brustenga et al. 2019) were

applied. Second, very short data lags of a few days were substituted by those generated by a kriging interpolation process (Stein 1999; Press et al. 2007) based on available daily records close to a gauge without data and the topography of the area around these emplacements. In this way, completeness of chosen monthly data was guaranteed. A length of 40 years, used in the previously mentioned papers, has been enlarged from 80 to 105 years for 11 available monthly records. A better analysis of changes on time trends along the beginning of the twentieth century up to nowadays is then available and some relationship between these changes and those detected on CO₂ increment emissions into the atmosphere can be analysed.

3 Climate characteristics

The climate of Catalonia (NE Spain) could be globally qualified as Mediterranean in agreement with the Köppen-Geiger classification (Mc Night and Hess 2000) with closeness to a warm sea (Western Mediterranean) and a notable distance to the Atlantic Ocean. Nevertheless, a notable variability due to a complex orography (Fig. 1a) must be considered. The most relevant mountain chains are the Pyrenees and Pre-Pyrenees at the North, Littoral and Pre-Littoral chains close to the Mediterranean coast and the Transversal chain. Additionally, it has to be also taken into consideration the Central Basin (SW of Catalonia). From the point of view of rainfall patterns and drought episodes, this orographic complexity and the atmospheric circulation patterns are basic factors governing the different rainfalls regimes in Catalonia. Western circulation from the Atlantic Ocean and Western and North-western circulations crossing the Pyrenees should be associated with episodes of scarce rainfall amounts (except for the north face of the Pyrenees). Low-pressure nuclei crossing Catalonia, which can be reactivated when they reach the Mediterranean sea, as well as Eastern advections, notably contribute to rainfall amounts. Additionally, convective phenomena, usually in summer, with flow of humid air masses from the Mediterranean and cold air masses at high levels, could generate copious and short rainfall episodes, interrupting drought episodes, but sometimes also causing floods (Lana et al. 2008; Pérez-Zanón et al. 2018; Llabrés-Brustenga et al. 2020).

In agreement with the exposed orographic and dynamic atmospheric variability, a single rainfall pattern for the whole domain of Catalonia has to be discarded. Two recent examples would be the multifractal analysis and the forecasting of monthly rainfall amounts (Lana et al. 2020a, 2021). Consequently, it is expected that several parameters quantifying the evolution of annual and monthly rainfall

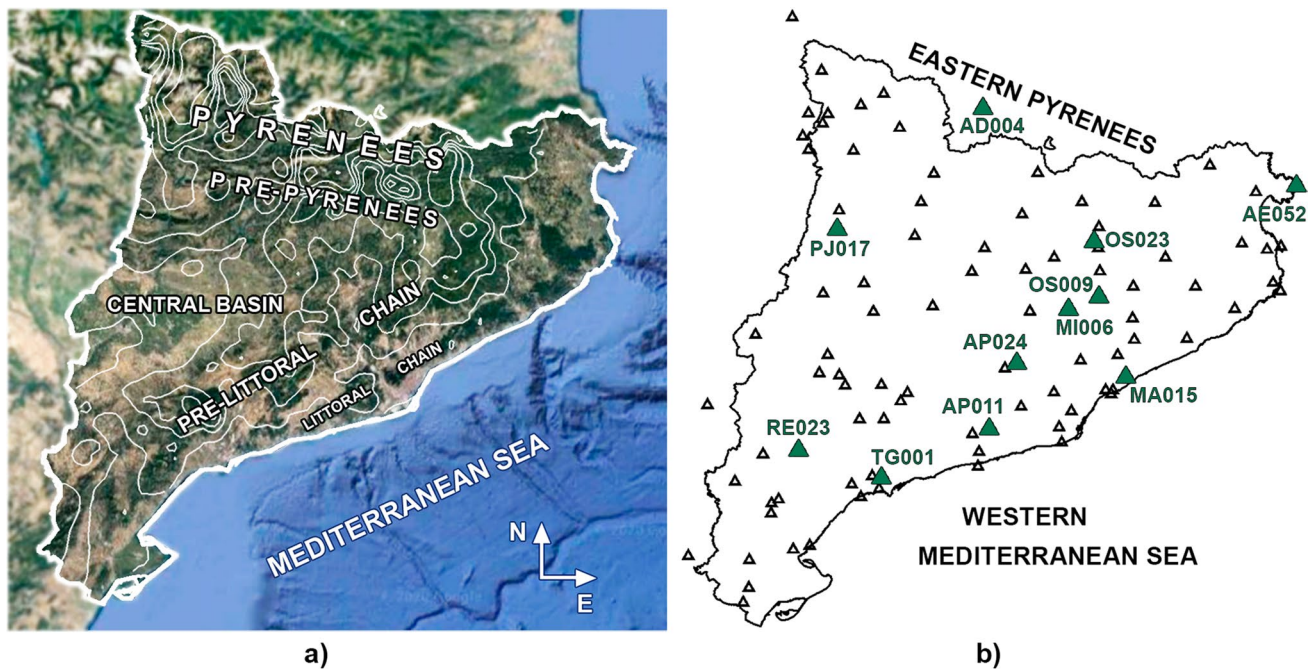


Fig. 1 **a** Schematic orography of Catalonia (NE Spain) and satellite photography. **b** Network of rain gauges, Catalonia (NE Spain). Bold green triangles correspond to the 11 rain gauges with record length equalling to or exceeding 85 years

amounts (time trends and their statistical significance, as well as irregularity of consecutive rainfall amounts) will depict a heterogeneous spatial distribution.

4 Evolution of monthly and annual amounts

The mentioned complex orography contributes to a heterogeneous spatial distribution of time trends at monthly and annual scales. A first approach to this heterogeneity is summarised in Table 1, where the predominance of monthly negative trends with statistical significance (Mann–Kendall test) equalling to or exceeding at least 85% is notable for winter and the beginning of spring (December, February and March) and exceptional in summer (June). Conversely, April is characterised by a predominance of positive time trends. The complex spatial distribution of time trends significance at monthly scale is shown in Fig. 2, where the thick black line delimits areas with statistical significance equalling to or exceeding 90%. It must be underlined that areas accomplishing this constraint increase or decrease along the year and that these nuclei change their geographic emplacement. Whereas the nuclei of high significance are dispersed in December, they are concentrated in the eastern Pyrenees (February), Western and NW Pyrenees (March), April (SW Catalonia) and covering a wide area of Catalonia in June. Five

examples of the monthly evolution (June) characterised by statistically significant negative time trends varying from -0.75 (maximum trend) to -0.22 mm/year (minimum trend) are depicted in Fig. 3. Given that these five series are included in the 11 samples of rain gauges with the longest records, these time trends and the smoothed

Table 1 Number of detected positive and negative monthly trends with statistically significant levels of 85, 90, 95 and 99%, in agreement with the Mann–Kendall test. Cases associated with positive and negative significant trends are detailed within parenthesis. The last column visualises the number of total statistical significant trends

	99% (+, -)	95% (+, -)	90% (+, -)	85% (+, -)	(+, -)
January	—	2 (1, 1)	—	—	(1, 1)
February	7 (0, 7)	7 (0, 7)	3 (0, 3)	12 (0, 12)	(0, 29)
March	7 (0, 7)	8 (0, 8)	7 (0, 7)	9 (0, 9)	(0, 31)
April	6 (6, 0)	6 (6, 0)	2 (1, 1)	6 (6, 0)	(19, 1)
May	1 (1, 0)	3 (1, 2)	2 (0, 2)	5 (1, 4)	(3, 8)
June	10 (0, 10)	23 (0, 23)	8 (0, 8)	9 (0, 9)	(0, 50)
July	2 (0, 2)	11 (5, 6)	3 (0, 3)	7 (0, 7)	(5, 18)
August	1 (0, 1)	2 (0, 2)	7 (0, 7)	5 (0, 5)	(0, 15)
September	2 (1, 1)	1 (1, 0)	6 (1, 5)	1 (0, 1)	(3, 7)
October	—	1 (0, 1)	3 (0, 3)	2 (1, 1)	(1, 5)
November	—	2 (1, 1)	4 (4, 0)	2 (2, 0)	(7, 1)
December	2 (0, 2)	6 (0, 6)	11 (0, 11)	12 (2, 12)	(2, 31)

evolution (thick black line) have been computed for a common interval of 65 years (1950–2015), becoming a good picture of these predominant monthly summer rainfall trends.

The evolution at annual scale of the pluviometric regime is described in Fig. 4, showing the spatial distribution of dispersed nuclei of statistical significance equalling or exceeding 90% and the spatial distribution of time trends.

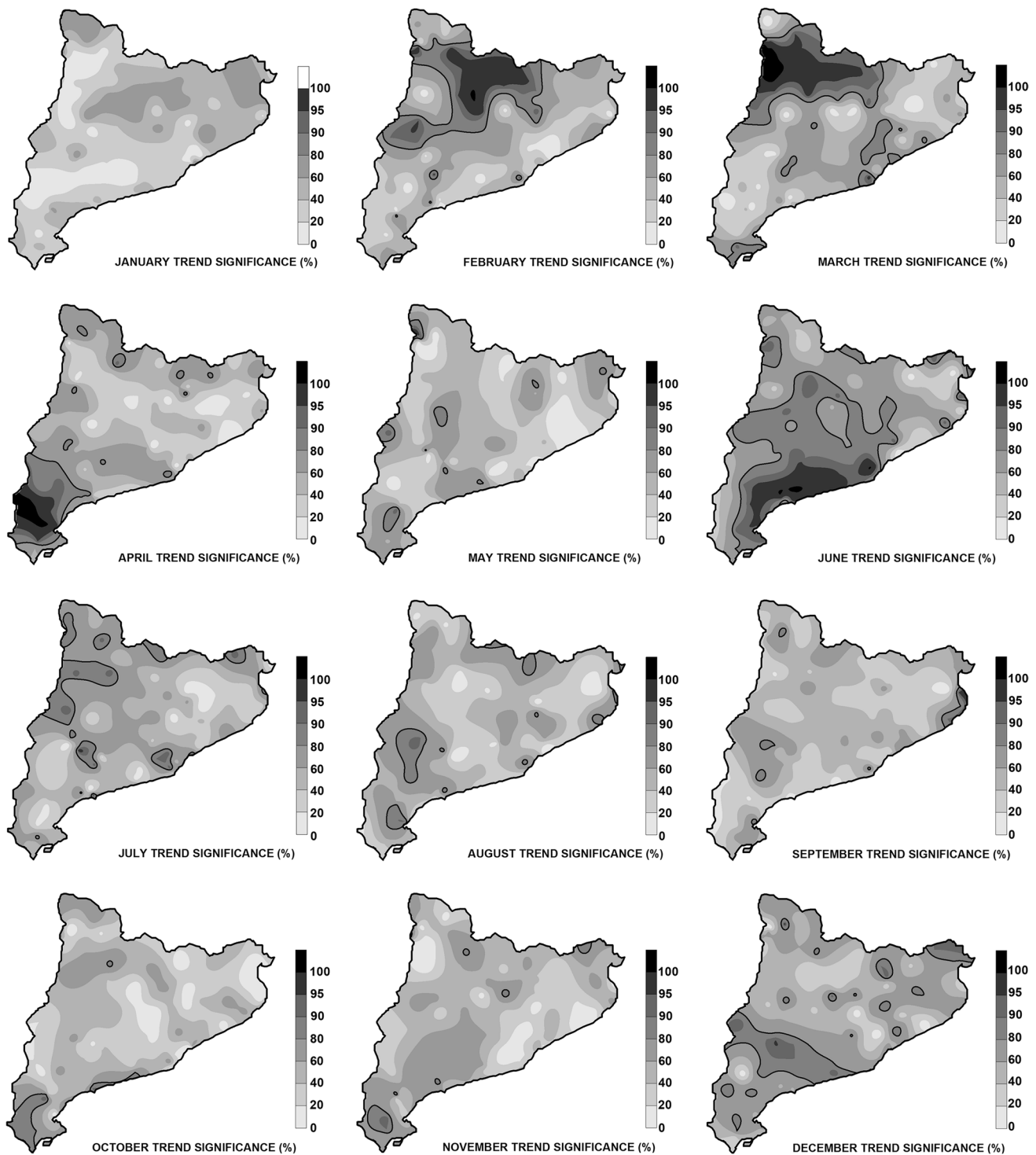


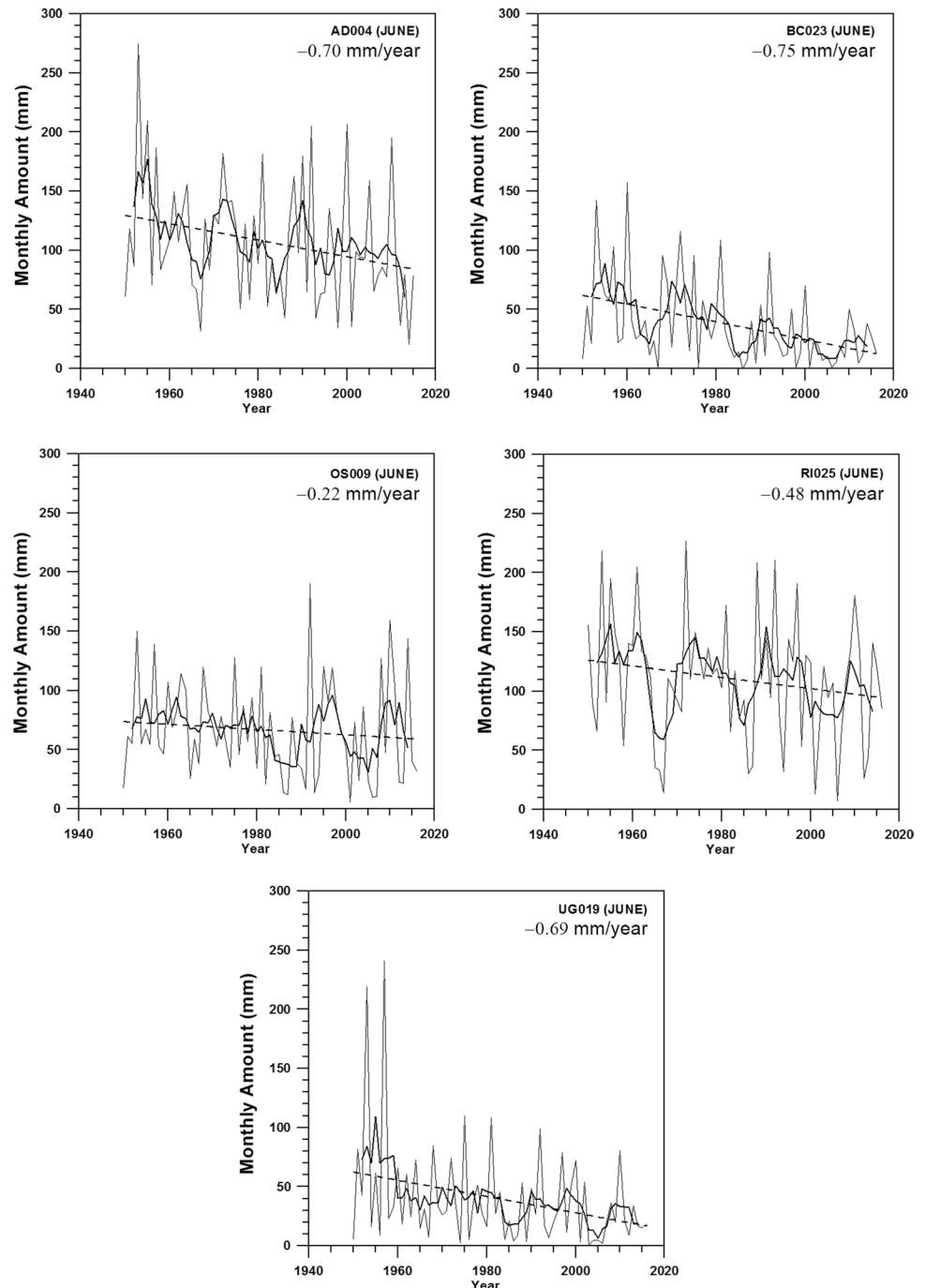
Fig. 2 Spatial distribution at monthly scale of time trends statistical significance. Thick black lines delimit areas where significance trends exceed 90%

Given that the annual statistical significance would be a superposition of the 12 monthly scales, the effects, for instance, of June time trends would be smoothed. Nevertheless, depending on the necessities of water supplies (agriculture, industry, potable water and hydroelectric power), both the usual rainfall amount oscillations along the year and the monthly and annual trends should be carefully considered. With respect to the time trends, it is worth mentioning two small nuclei with high negative time trends (5–10 mm/year), another disperse areas with positive time trends (0–5 mm/

year) and a clear predominance of moderate negative time trends (less than 5 mm/year). The results concerning these annual time trends are not negligible bearing in mind that they have been computed for a common recording length of 40 years. Consequently, the dominant negative time trends (0–5 mm/years) would represent a maximum reduction of 200 mm along the last 40 years.

A more complete point of view of this decreasing tendency on the rainfall amounts can be obtained by taking advantage of the available 11 rain gauge records exceeding

Fig. 3 Several examples of monthly amounts evolution for June, which is the month with the highest number of detected statistically significant trends. Thin and thick lines respectively depict the annual evolution of June amounts and the smoothed profile of this evolution. Dashed line describes the time trend



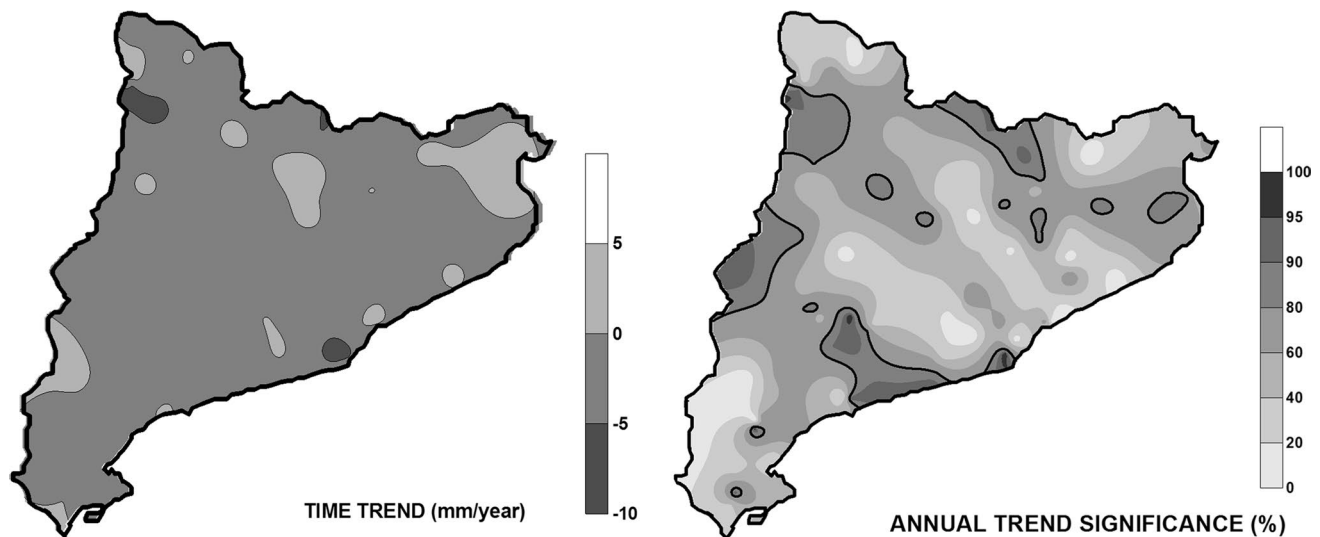


Fig. 4 Spatial distribution of annual trends and their statistical significance

85 years. Figure 5 depicts the evolution of these records, being detected only three positive trends (gauges MI006, PJ017 and RE023) which change to negative when the time trends are computed for years 1950(1960)–2015. Consequently, 8 available long recorded data covering a good part of the twentieth century up to nowadays depict negative time trends and the other three examples of positive time trends change to negative when the last 55–65 years are analysed. Then, the behaviour of the 96 rain gauges for the last 40 years, with a high percentage of monthly and annual negative time trends, is reinforced by the comparison with the longest records exceeding 80 years. In agreement with these results, besides monthly patterns characterised by increasing and decreasing trends, a reduction of annual rainfall amounts could be expected along the twenty-first century. This possibility could be in agreement with the evolution of CO₂ emissions (<https://www.statista.com>) and the corresponding increment of remaining CO₂ into the atmosphere (Meinshausen et al. 2017).

Another relevant question is the degree of irregularity of the annual series, based on concepts of disparity and fractal analysis. Different parameters associated with this possible irregularity are considered, three of them based on the concepts of variability and general and specific disparity parameters. A detailed description and definition of these three parameters, as well as their application to the annual rainfall regime of the southwestern Iberian Peninsula, can be found in García-Barrón et al. (2011). The first parameter is a running variation coefficient,

$$CVAR(i) = \frac{\sigma(i, \gamma)}{\mu(i, \gamma)} \quad (1)$$

with average and standard deviation computed for consecutive segments of $\gamma = 11$ years, this length segment being chosen in agreement with the well-known periodicity on rainfall amount series $\{P_i\}$ and the concordance with the periodicity of the solar activity (Cameron and Schüssler 2019). A general disparity index, GDI

$$GDI = \frac{1}{\mu} \left\{ \sum_i (P_{i+1} - P_i)^2 / (n - 1) \right\}^{1/2} \quad (2)$$

for every complete annual series is also computed, which is based on the cumulated square discrepancies between consecutive annual amounts divided by the average μ of all the available annual amounts. This index only offers a global point of view of the irregularity and a specific disparity index; SDI is also convenient, offering a more detailed description of the irregularity evolution, being also interesting to analyse the maximum and minimum SDI values for every annual rainfall series, searching for some relationship between these SDI extremes and the rainfall average for the whole set of annual data. This last index is computed by taking into account three consecutive annual amounts for every year i (P_{i-1} , P_i , P_{i+1}), being added the square discrepancies for pairs (P_{i-1} , P_i) and (P_i , P_{i+1}) and after that divided by the average, $\mu(i)$, of the three corresponding consecutive annual amounts

$$SDI = \frac{1}{2^{1/2} \mu(i)} \left\{ (P_{i+1} - P_i)^2 + (P_i - P_{i-1})^2 \right\}^{1/2} \quad (3)$$

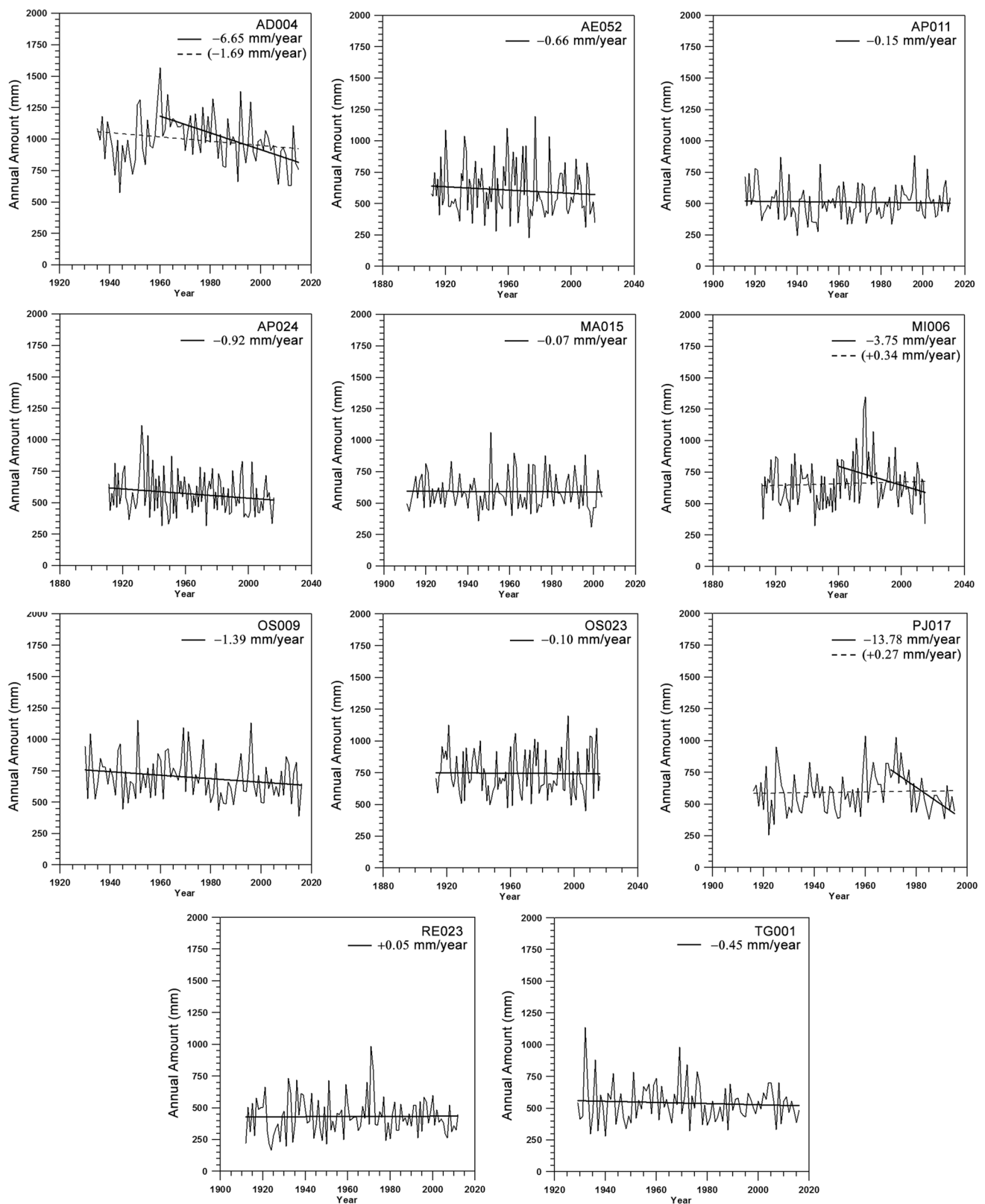


Fig. 5 Annual amount evolution for the longest annual records exceeding 80 years. Three time trends (gauges AD004, MI006 and PJ017) detected since 1960 notably differ with respect to those obtained for the whole available records

Another parameter related with the degree of irregularity is a scaling exponent which has been also associated with CO₂ increases (Lana et al. 2021). The scale properties of rain can be expressed through statistical relationships that describe its fractal behaviour (Schertzer and Lovejoy 1987). The statistical moments of the probability distribution of the annual maximum rainfall intensity I_t for a duration t can be related to the moments of the corresponding distribution on another scale λt using the scaling relationship (Burlando and Rosso 1996; Menabde et al. 1999).

$$\langle I_t^q \rangle = \lambda^{\beta q} \langle I_{\lambda t}^q \rangle \quad (4)$$

A relationship between the values of the scaling exponent β and the characteristics of the rainfall pattern of the place of study has been reported (Rodríguez-Solà et al. 2017; Casas-Castillo et al. 2018a, b). In rainy areas, where synoptic rain is usually prevailing, the parameter β usually gets the lowest absolute values. On the other hand, in other zones with a more irregular rainfall regime, which are usually drier and sometimes present a notable proportion of convective rainfall, the absolute value of this parameter is higher.

With the aim of guaranteeing a quality of the results obtained with the four irregularity parameters, only the irregularity for the longest 11 annual records, covering a minimum of 85 consecutive years and without gaps, has been computed. Table 2 summarises the results obtained for parameters GDI; the average annual amount, μ , for every complete series; the extreme maximum and minimum values of the parameters CVAR and SDI; and the fractal single scaling parameter β . The parameter GDI offers a global overview for every annual series, being detected signs of regularity (relatively small GDI and moderate β values) for gauges AD004 and OS023 on the mountainous area of the Pyrenees and Pre-Pyrenees, with the highest averaged annual amounts. The very similar values of minimum CVAR close to zero suggest that the 11 annual series are characterised by some intervals of

regularity (low standard deviations in comparison with the corresponding average amounts). The maximum values of CVAR lowering 0.80 (gauges AD004, OS023 and MI006) associated with moderate irregularity are characterised by mean annual amounts of 991.8, 747.0 and 658.2 mm, respectively, which could be qualified as relatively copious, especially the gauge AD004, and of moderate rainfall regimes, in comparison with a standard Mediterranean rainfall regime. CVAR maxima values exceed 0.8, sometimes close to or exceeding 1.0, for the other 8 gauges. It is worth mentioning that for six of these annual series, the mean annual amounts do not exceed 600 mm and it is noticeable the highest maximum CVAR (1.08) assigned to gauge RE023 with a mean annual amount of only 432.6 mm.

An additional characterisation of the irregularity is obtained by the parameter SDI. The minimum values of this parameter do not exceed 0.21, suggesting that for some windows of 3 consecutive years, the irregularity is small. An example of notably low irregularity would be again the gauge AD004 ($\text{SDI}_{\min} = 0.09$) with a mean annual amount of 991.8 mm. With respect to the maximum values of SDI, it is noticeable that gauges AD004 and OS023 are characterised again by moderate irregularity, with parameters equalling to or lowering 0.30. It is relevant to remember that these two rain gauges could be also characterised by low irregularity in agreement with the maxima of CVAR parameter.

The increase or decrease of rainfall irregularity can be quantified by revising the time trends of CVAR and SDI for years (1960–2010). Only CVAR annual series for gauges AD004, AP024 and OS023 depict small positive time trends (9.6×10^{-4} , 1.69×10^{-3} and $7.90 \times 10^{-4} \text{ year}^{-1}$, respectively). For the other 8 records, the CVAR trends are negative and slightly higher, varying from -0.68×10^{-4} (AP011) to $-3.54 \times 10^{-3} \text{ year}^{-1}$ (RE023). With respect to the SDI parameter, only a small positive trend ($7.22 \times 10^{-5} \text{ year}^{-1}$) is detected again for gauge AD004. All the other 10 SDI curves are characterised by negative time trends for

Table 2 General disparity index, GDI, average annual amount, μ (mm/year), maximum and minimum values of the specific disparity index, SDI, and the long-term variability, CVAR, and the scaling parameter β

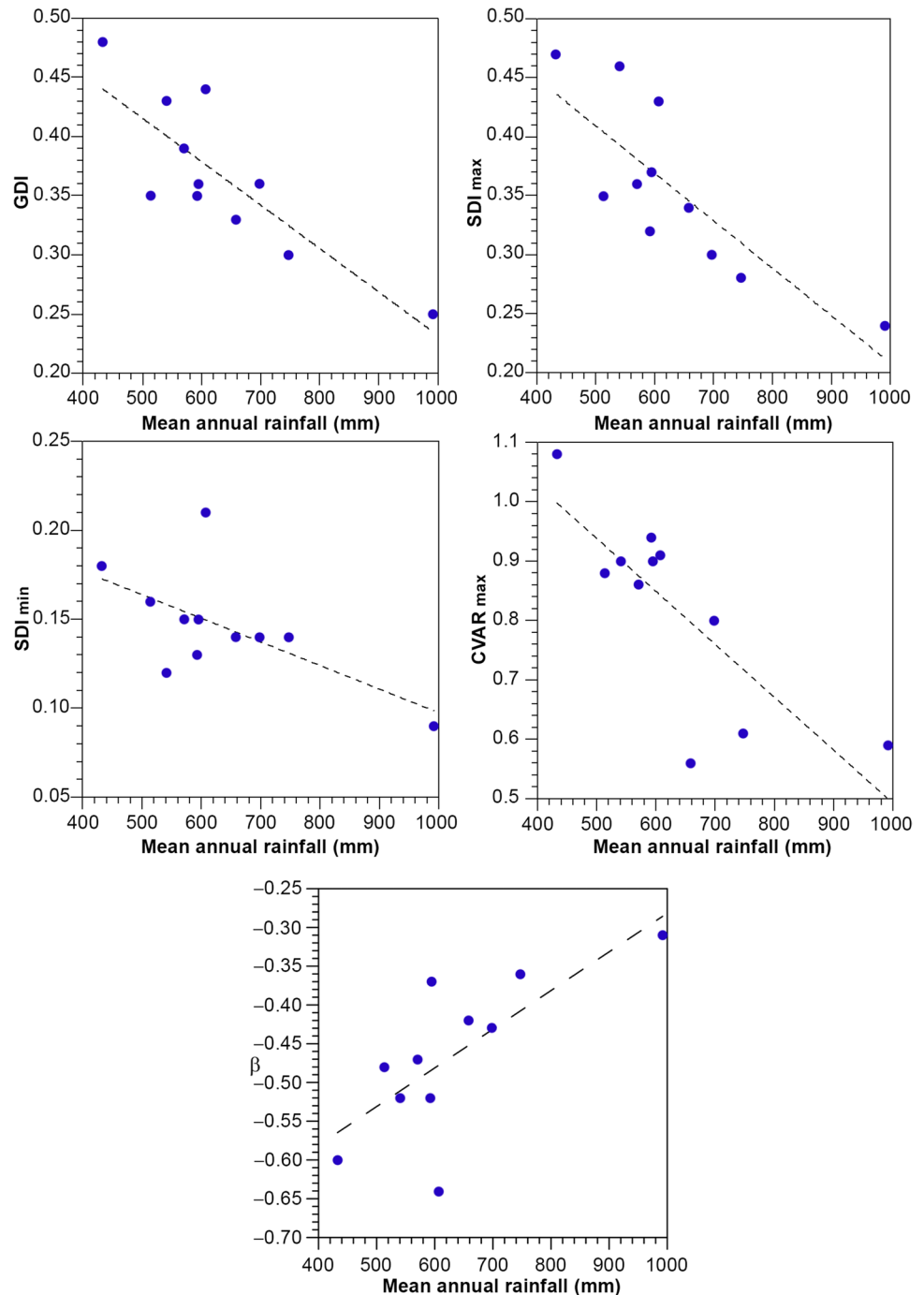
Gauge	GDI	μ	SDI(max)	SDI(min)	CVAR(max)	CVAR(min)	β
AD004	0.25	991.8	0.24	0.09	0.59	0.02	−0.31
AE052	0.44	607.1	0.43	0.21	0.91	0.05	−0.64
AP011	0.35	513.5	0.35	0.16	0.88	0.01	−0.48
AP024	0.39	570.5	0.36	0.15	0.86	0.04	−0.47
MA015	0.35	592.4	0.32	0.13	0.94	0.03	−0.52
MI006	0.33	658.2	0.34	0.14	0.56	0.01	−0.42
OS009	0.36	697.9	0.30	0.14	0.80	0.06	−0.43
OS023	0.30	747.0	0.28	0.14	0.61	0.01	−0.36
PJ017	0.35	594.8	0.37	0.15	0.90	0.30	−0.37
RE023	0.48	432.6	0.47	0.18	1.08	0.02	−0.60
TG001	0.43	541.0	0.46	0.12	0.90	0.04	−0.52

years (1960–2010) varying from -8.51×10^{-5} (RE023) to -5.77×10^{-3} (AE052). In agreement with the time trends obtained for CVAR and SDI, the changes on the rainfall irregularity are expected to be small for the forthcoming years, becoming more relevant the diminishing tendency of annual rainfall amounts.

The scale parameter β (Table 2) has been computed by taking sliding intervals of 50 years, varying the temporal range in 1 year and covering the rainfall records since the beginning of the twentieth century up to nowadays. This

fractal parameter shows a consistent behaviour with the previous parameters. The highest values of the parameter are found in the mountainous areas of the Pyrenees and Pre-Pyrenees—AD004 (−0.31), OS0023 (−0.36) and PJ017 (−0.37)—while in the northern and southern coastal areas, the lowest values of the scale parameters are found, AE052 (−0.64) and RE023 (−0.60), corresponding to places with high irregularity. The very negative value of the parameter β obtained for AE052 (at the northeast coast) could not be a dry zone with scarce rainfall, given that its average annual

Fig. 6 Dependence of the parameters GDI, maximum and minimum SDI, maximum CVAR and scaling parameter β on the mean annual rainfall



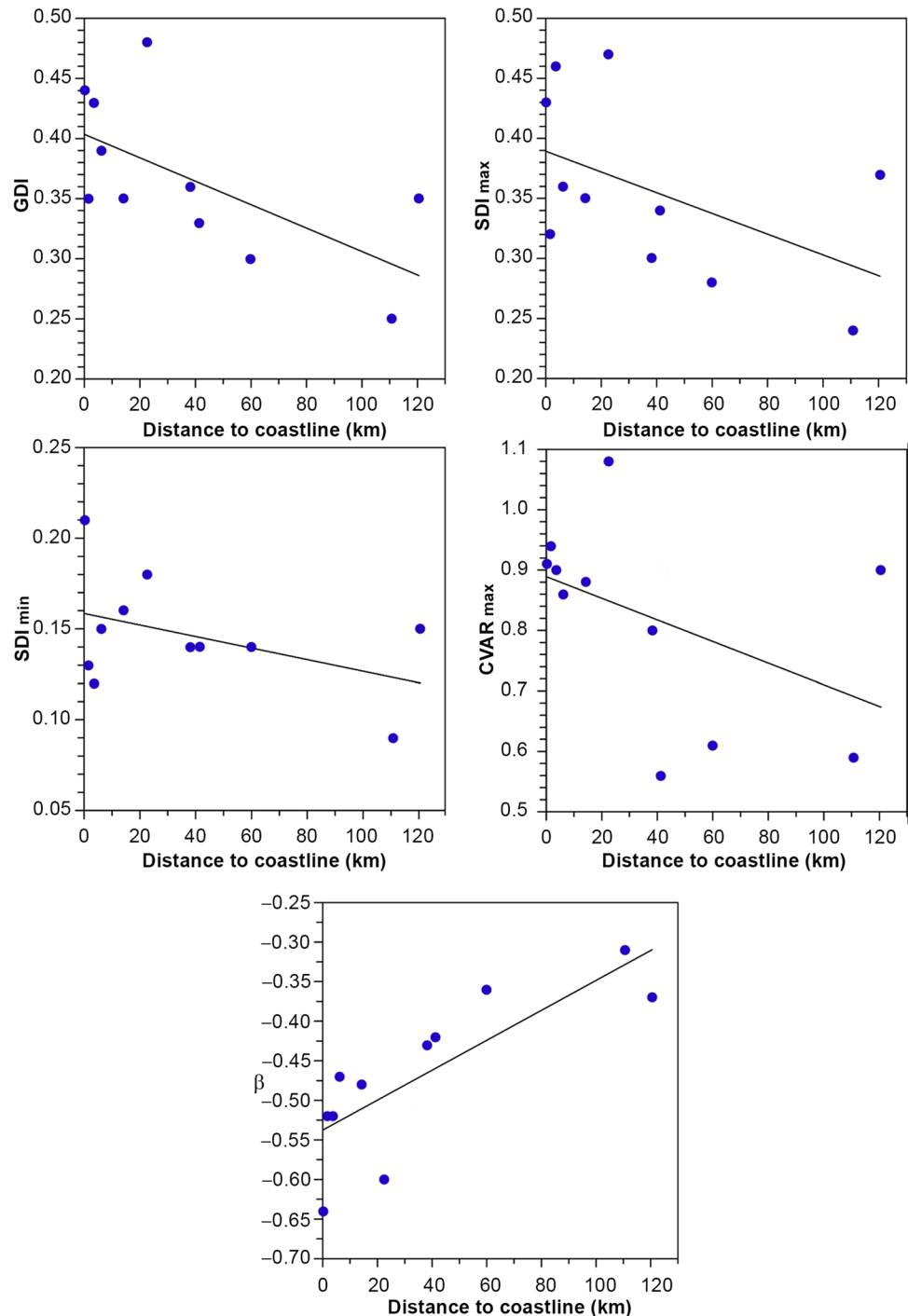
precipitation is 607.1 mm, but it can be explained due to its irregular rainfall regime. For instance, the highest daily rainfall recorded in Catalonia (430 mm on October 13, 1986) corresponds to this rain gauge.

Some kind of correlation between the parameters quantifying irregularity and the mean annual rainfall, μ , could be expected in agreement with Fig. 6. The values of the parameters GDI , SDI_{\max} , SDI_{\min} and $CVAR_{\max}$ depict a tendency to diminish when μ increases, being then reduced the

irregularity degree. Additionally, the absolute value of β also decreases with the increase of μ , diminishing the irregularity. In spite of an accurate mathematical dependence of these parameters on the mean annual rainfall is difficult to stablish, a tendency to diminish the irregularity for an increase on annual amounts is quite evident.

The distance to the coastline could be another important factor for the rainfall irregularity. In the coastal area, even though mean annual rainfall could be moderate, heavy rain

Fig. 7 Dependence of the parameters GDI , the maximum and minimum SDI , maximum $CVAR$ and scaling parameter β on the distance to the coastline



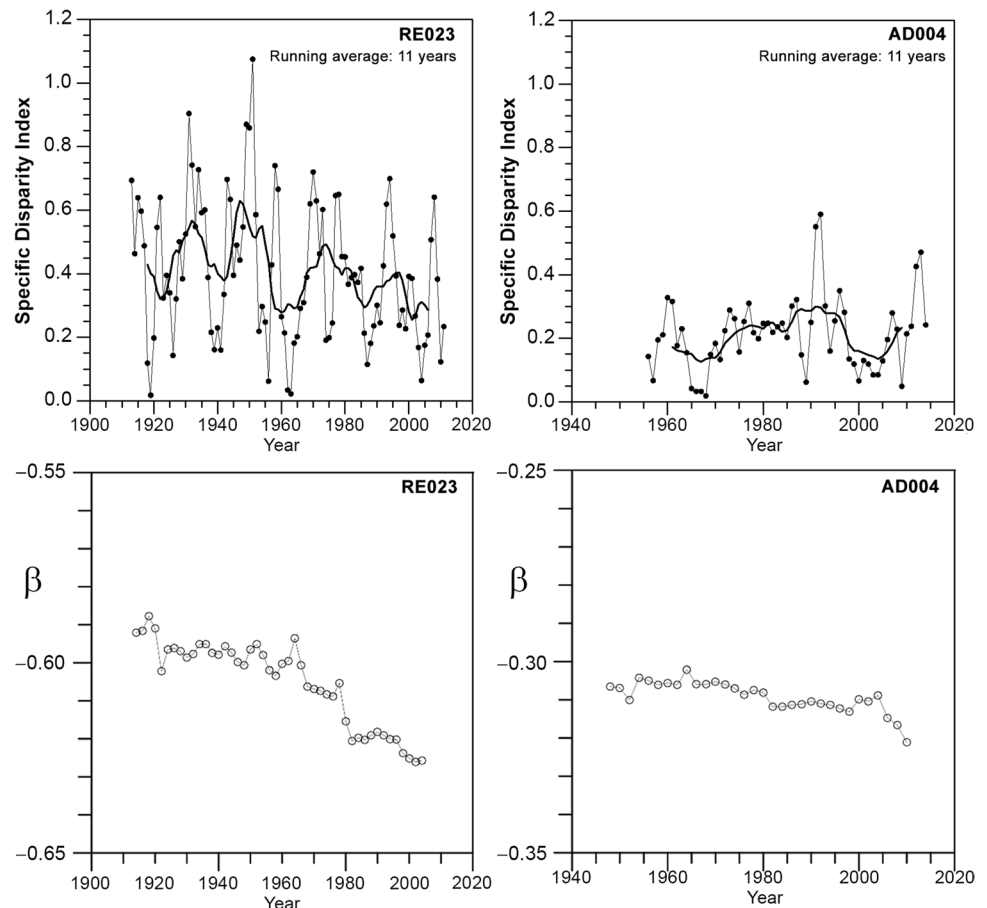
episodes associated to Mediterranean low-pressure systems bringing wet eastern winds often occur (Casas-Castillo et al. 2018a), contributing to the rainfall irregularity. A possible dependence of the irregularity parameters GDI , SDI_{max} , SDI_{min} and $CVAR_{max}$ and the fractal parameter β on the distance to the Mediterranean coastline is depicted in Fig. 7. In spite of this dependence is not very clear for parameters GDI , SDI_{max} , SDI_{min} and $CVAR$, the relationship between distance and parameter β is quite evident.

Two additional illustrative examples of the dependence of the irregularity on the annual amount, with very different annual amounts and distance to the littoral chain, are shown in Fig. 8. The evolution of SDI for gauge RE023, with the lowest annual amount and very close to the Mediterranean coast, is very different to that corresponding to gauge AD004, with the highest annual amount and emplaced in the Eastern Pyrenees. Whereas for AD004 series, the SDI coefficient is close to 0.2, it ranges from 0.2 to 0.4 for gauge RE023. With respect to the fractal coefficient β , both tendencies are negative, increasing the irregularity, being worth mentioning a higher increasing of irregularity for gauge RE023 (≈ 0.60) in comparison with gauge AD004 (≈ 0.30).

5 The possible effects of CO₂ emissions

Nowadays, given that the greenhouse phenomenon generated by excessive CO₂ emissions into the atmosphere, as well as by other compounds as methane gas, is absolutely accepted, quite evident influences on thermometric regimes, but also on pluviometric regimes, have to be accepted. Several examples of the temperature regime changes, at different geographic scales and due to greenhouse gases effects, are Bloomfield (1992), Stern and Kaufmann (2000), Jones and Moberg (2003), Sigró et al. (2005), Gil-Alana (2009) and Gil-Alana and Sauci (2019), among others. The increasing greenhouse gases could also affect the pluviometric regimes, changing rainfall patterns leading to extreme episodes, increasing of flood risks or variations on IDF curves (Mansell 1997; Arnbjerg-Nielsen et al. 2013; Mirhosseini et al. 2013; Rodríguez et al. 2014; Liuzzo and Freni 2015; among others). Additionally, questions such as increment of forest fire risk (Huber 2018) or agricultural problems due to increments of drought episodes in semi-arid areas (Miranda et al. 2011) could also be consequence of a reduction of rainfall amounts due to the climatic change. The increasing annual emission of CO₂ into the atmosphere for a long time up to nowadays can be found in <https://www.statista.com> (Hamburg-Germany) and the annual evolution of remaining

Fig. 8 Two examples of the very different evolution of the parameter SDI and the scaling parameter β for gauges RE023 and AD004. Thick line depicts the running average of SDI



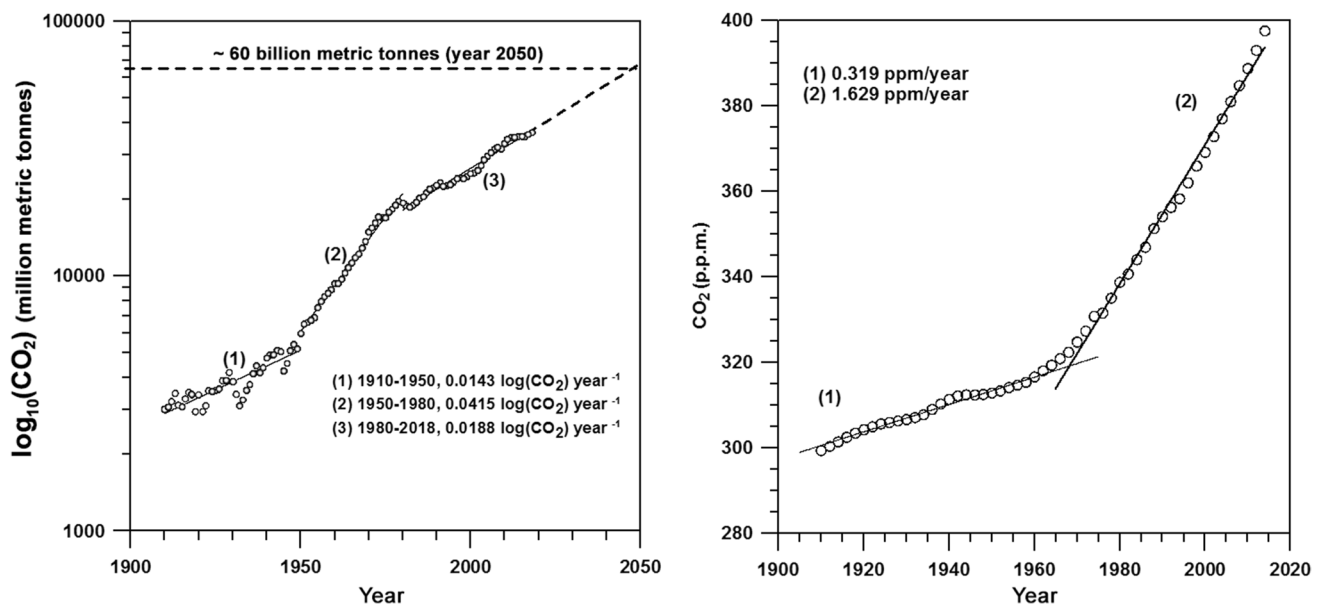


Fig. 9 Evolution at annual scale of CO₂ emissions and concentration of this greenhouse gas into the atmosphere (1910–2018)

CO₂ into the atmosphere has been evaluated by Meinshausen et al. (2017). An example of the CO₂ effects on the Mediterranean region could be the reduction of the annual amounts, in agreement with the negative time trends detected in this paper, the increasing of extreme episodes and the perseverance of long drought episodes (Pérez and Boscolo 2010; Miranda et al. 2011). Another factor to be considered is the increase of the rainfall irregularity at monthly scale detected by Lana et al. (2021) by means of fractal analysis and with a remarkable relationship with CO₂ emissions. The increasing emission of CO₂ since 1910 up to nowadays is schematised in Fig. 9 by three different logarithmic evolutions. Whereas the first and third evolution (1910–1950 and 1980–2018) are characterised by very similar increasing slopes, the second evolution (1950–1980) manifests a higher slope with respect to the others. Assuming the slope of emissions would not change after 2018, a quantity close to 60×10^9 metric tonnes (year 2050) could not be discarded, a high value which could notably affect the pluviometric regime. The permanence of injected CO₂ into the atmosphere, in p.p.m. units, since 1910 up to nowadays is also represented in Fig. 9. In this case, the evolution is characterised by two well-defined linear evolutions. The first one (1910–1960) is almost coincident with the years interval corresponding to the first slope of CO₂ emissions into the atmosphere and the second, notably higher in comparison with the first, covering the years associated with the second and third slope of CO₂ emissions. The continuity without changes of this second slope suggests a concentration close to 450 p.p.m. in 2050.

One of the probable effects of CO₂ emissions on pluviometric regimes, in agreement with Büntgen et al. (2021), is an increment of drought severity, compatible with rainfall irregularity and negative time trends. These authors, after analysing tree-ring stable carbon and oxygen isotopes from more than 100 samples (oaks tree), finally assumed that droughts since 2015 are unprecedented comparing with the previous 2100 years. These authors suggested that this climatic anomaly could be consequence of anthropogenic processes (CO₂ emissions, among others) and of the atmosphere dynamics (changes on summer jet stream). This atmospheric dynamic change on summer would be coherent with the

Table 3 Recorded length, lag (years) for CO₂ and annual amounts cross-correlations, time trend (mm/year) and statistical significance for 11 annual rainfall series exceeding records of 80 years. Notable changes on time trends (within parenthesis) are those detected since 1960 for gauges AD004, MI006 and PJ107

Gauge	Years	Pearson	Lag	Time trend	MK (%)
AD004	81	−0.25	33	−1.69 (−6.65)	95 (99)
AE052	105	−0.13	44	−0.66	70
AP011	99	+0.02	22	−0.15	5
AP024	106	−0.18	53	−0.92	85
MA015	94	−0.01	18	−0.07	40
MI006	105	+0.05	31	+0.34 (−3.75)	35 (95)
OS009	87	+0.21	39	−1.39	90
OS023	104	+0.03	39	−0.10	35
PJ017	80	+0.02	18	+0.27 (−13.78)	15 (99)
RE023	101	−0.03	40	+0.05	10
TG001	88	−0.08	44	−0.45	5

detected high number of rain gauges characterised by statistically significant negative time trends in June (Table 1) and at annual scale for the longest 11 annual records (Table 3). Additionally, a possible correlation between annual amounts and increase of permanent CO₂ in atmosphere has to be analysed, bearing in mind the cross-correlation lag between both variables. With the aim of improving the veracity of cross-correlation results, only the 11 annual series exceeding 80 years record length have been considered. Cross-correlation lags could be expected quite similar for the 11 records, given that the CO₂ emissions globally affect all the analysed area. Nevertheless, the effects of greenhouse gases on the

rainfall regime could be slightly different due to the complex orography of Catalonia. Table 3 summarises the obtained results and some examples of cross-correlation evolution are shown in Fig. 10. The 11 very moderate Pearson coefficients vary from -0.25 (gauge AD004) to $+0.21$ (gauge OS009), suggesting a not very remarkable dependence of annual rainfall amounts on the CO₂ evolution. Nevertheless, the negative time trends are notably predominant, especially for the last 50–60 years, being noticeable the change from positive to negative trends for gauges MI006 and PJ017. Only gauge RE023 is characterised by a positive time trend, very close to zero and with low statistical significance. The

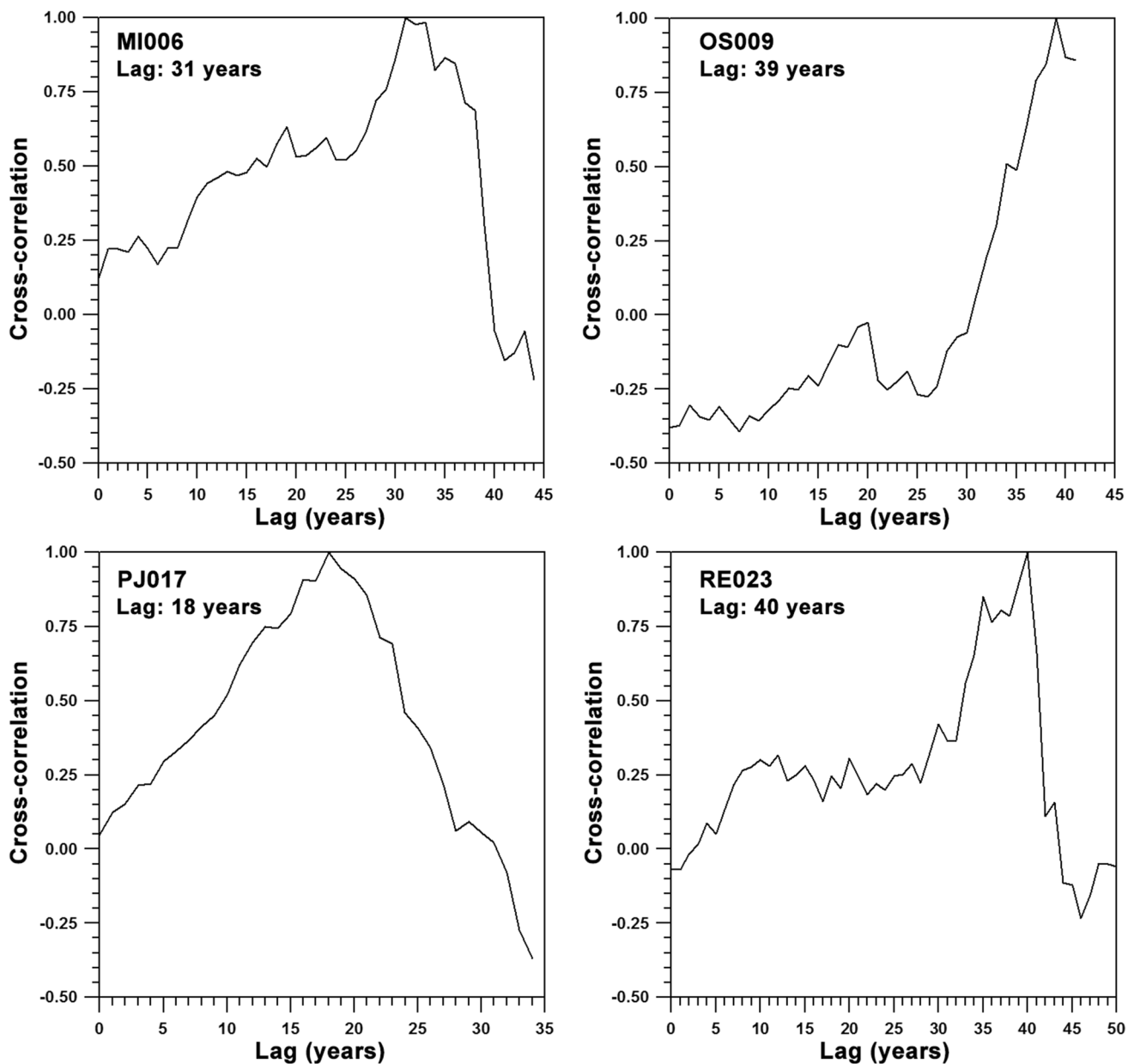


Fig. 10 Some examples of annual amounts and CO₂ emissions cross-correlation (1910–2018)

list of annual lags (Table 3) reinforces the hypothesis of a low dependence of annual amounts on CO₂ emission increment. Bearing in mind these lags vary within a wide range from 18 to 53 years, it becomes difficult to assume a clear dependence on CO₂ emissions.

6 Conclusions

The heterogeneous spatial distribution of rainfall time trends at monthly and annual scales and the corresponding statistic significances and irregularity coefficients are in agreement with the complex orography of Catalonia. In this way, a single pattern of rainfall time evolution for the whole Catalonia (NE Spain) is not possible. The vicinity to Pyrenees and other mountain chains, as well as to the Mediterranean coast, notably conditions the evolution of rainfall amounts. Despite this shortcoming, a global evolution towards minor annual amounts is detected, with some opposite trends at monthly scale and different trend magnitudes. This tendency to the reduction of annual amounts is specially observed for the 11 longest records exceeding 85 years, with only one case of positive trend very close to zero and the other 10 records depicting negative trends, some of them quite relevant.

In short, the future pluviometric regime in Catalonia (NE Spain) should be characterised by two factors: first, a notable spatial variability of rainfall time trends at monthly and annual scales, most of them negative and statistically significant, and second, the persistence of annual rainfall irregularity, with signs of dependence on the distance to the Mediterranean coastline and average annual rainfall amounts. Additionally, the evolution of the annual amounts depending on the emission and permanence of CO₂ into the atmosphere shows some affirmative signs. Nevertheless, the cross-correlation lag and Pearson coefficient results do not contribute to a clear answer to this question.

Acknowledgements Rainfall data have been supplied by Servei Meteorològic de Catalunya (Generalitat de Catalunya), Fabra Observatory (RACA, Barcelona) and Ebro Observatory (Ramón Llull University and CSIC, Spanish Government). This research was supported by the Spanish Ministry of Science, Innovation and Universities: grant 460 number PID2019-105976RB-I00] and grant number AGL2017-87658-R. The authors also thank the editor and the anonymous reviewers for their valuable comments and suggestions to improve the manuscript.

Author contribution All authors contributed to the study conception and design. Material preparation, data collection and analysis were performed by Ricard Kirchner, Xavier Lana, Raül Rodríguez-Solà and M. Carmen Casas-Castillo. The first draft of the manuscript was written by Xavier Lana and all authors commented on previous versions of the manuscript. All authors read and approved the final manuscript.

Funding Open Access funding provided thanks to the CRUE-CSIC agreement with Springer Nature. This research has been financed by

the project PID2019-105976RB-I00 (Agencia Estatal de Investigación, Spanish Government).

Data availability Rainfall data used to support the findings of this study were supplied by Servei Meteorològic de Catalunya (Generalitat de Catalunya), available by request to dades.meteocat@gencat.cat.

Code availability Not applicable.

Declarations

Ethics approval Not applicable.

Consent to participate All authors consent to participate into the study.

Consent for publication All authors consent to publish the study in a journal article.

Conflict of interest On behalf of all authors, the corresponding author declares no competing interests.

Open Access This article is licensed under a Creative Commons Attribution 4.0 International License, which permits use, sharing, adaptation, distribution and reproduction in any medium or format, as long as you give appropriate credit to the original author(s) and the source, provide a link to the Creative Commons licence, and indicate if changes were made. The images or other third party material in this article are included in the article's Creative Commons licence, unless indicated otherwise in a credit line to the material. If material is not included in the article's Creative Commons licence and your intended use is not permitted by statutory regulation or exceeds the permitted use, you will need to obtain permission directly from the copyright holder. To view a copy of this licence, visit <http://creativecommons.org/licenses/by/4.0/>.

References

- Arnbjerg-Nielsen K, Willems P, Olsson J, Beecham S, Pathirana A, Bülow Gregersen I, Madsen H, Nguyen VTV (2013) Impacts of climate change on rainfall extremes and urban drainage systems: a review. *Water Sci Technol* 68:16–28. <https://doi.org/10.2166/wst.2013.251>
- Bloomfield P (1992) Trends in global temperature. *Clim Change* 21:1–16. <https://doi.org/10.1007/BF00143250>
- Büntgen U, Urban O, Krusic PJ, Rybníček M, Kolář T, Kyncl T, Ač A, Koňasová E, Čáslavský J, Esper J, Wagner S, Saurer M, Tegel W, Dobrovolný P, Cherubini P, Reinig F, Trnka M (2021) Recent European drought extremes beyond Common Era background variability. *Nature Geoscience* 14:190–196. <https://doi.org/10.1038/s41561-021-00698-0> <https://www.nature.com/articles/s41561-021-00698-0>
- Burlando P, Rosso R (1996) Scaling and multiscaling models of depth-duration-frequency curves for storm precipitation. *J Hydrol* 187:45–64. [https://doi.org/10.1016/S0022-1694\(96\)03086-7](https://doi.org/10.1016/S0022-1694(96)03086-7)
- Cameron RH, Schüssler M (2019) Solar activity: periodicities beyond 11 years are consistent with random forcing. *Astron Astrophys* 625:A28. <https://doi.org/10.1051/0004-6361/201935290>
- Casas MC, Herrero M, Ninyerola M, Pons X, Rodríguez R, Rius A, Redaño Á (2007) Analysis and objective mapping of extreme daily rainfall in Catalonia. *Int J Climatol* 27:399–409. <https://doi.org/10.1002/joc.1402>
- Casas-Castillo MC, Llabrés-Brustenga A, Rius A, Rodríguez-Solà R, Navarro X (2018a) A single scaling parameter as a first

- approximation to describe the rainfall pattern of a place: application on Catalonia. *Acta Geophys* 66(3):415–424. <https://doi.org/10.1007/s11600-018-0122-5>
- Casas-Castillo MC, Rodríguez-Solà R, Navarro X, Russo B, Lastra A, González P, Redaño A (2018b) On the consideration of scaling properties of extreme rainfall in Madrid (Spain) for developing a generalized intensity-duration-frequency equation and assessing probable maximum precipitation estimates. *Theor Appl Climatol* 131(1–2):573–580. <https://doi.org/10.1007/s00704-016-1998-0>
- García-Barrón L, Aguilar M, Sousa A (2011) Evolution of annual rainfall irregularity in the southwest of the Iberian Peninsula. *Theoret Appl Climatol* 103:13–26. <https://doi.org/10.1007/s00704-010-0280-0>
- Gil-Alana LA (2009) Persistence and time trends in the temperatures in Spain. *Advances in Meteorology*, Article ID 415290 <https://doi.org/10.1155/2009/415290>
- Gil-Alana LA, Sauci L (2019) Temperature across Europe: evidence of time trends. *Clim Change* 157:355–364. <https://doi.org/10.1007/s10584-019-02568-6>
- Huber K (2018) Resilience strategies for wildfire. The Center for Climate and Energy Solution. C2ES.org, November 2018, 1–12. Arlington, USA. Available at: <https://www.c2es.org/wp-content/uploads/2018/11/resilience-strategies-for-wildfire.pdf>
- Jones PD, Moberg A (2003) Hemispheric and large-scale surface air temperature variations: an extensive revision and an update to 2001. *J Clim* 16:206–223. [https://doi.org/10.1175/1520-0442\(2003\)016%3c0206:HALSSA%3e2.0.CO;2](https://doi.org/10.1175/1520-0442(2003)016%3c0206:HALSSA%3e2.0.CO;2)
- Lana X, Burgueño A (1998) Spatial and temporal characterization of annual extreme droughts in Catalunya (NE Spain). *Int J Climatol* 18:93–110. [https://doi.org/10.1002/\(SICI\)1097-0088\(199801\)18:1<93::AID-JOC219>3.0.CO;2-T](https://doi.org/10.1002/(SICI)1097-0088(199801)18:1<93::AID-JOC219>3.0.CO;2-T)
- Lana X, Serra C, Burgueño A (2001) Patterns of monthly rainfall shortage and excess in terms of the standardized precipitation index for Catalonia (NE Spain). *Int J Climatol* 21:1669–1691. <https://doi.org/10.1002/joc.697>
- Lana X, Martínez MD, Serra C, Burgueño A (2004) Spatial and temporal variability of the daily rainfall regime for Catalonia (NE Spain), 1950–2000. *Int J Climatol* 24:613–641. <https://doi.org/10.1002/joc.1020>
- Lana X, Burgueño A, Martínez MD, Serra C (2008) A review of dry spells statistics in Catalonia (NE Spain). In *droughts: cause, effects and predictions*, 191–218. Editor: J.M. Sánchez. Nova Science Publishers Inc., New York. ISBN 978–1–60456–285–9.
- Lana X, Casas-Castillo MC, Serra C, Rodríguez-Solà R, Redaño A, Burgueño A, Martínez MD (2019) Return period curves for extreme 5-min rainfall amounts at the Barcelona urban network. *Theoret Appl Climatol* 135:1243–1257. <https://doi.org/10.1007/s00704-018-2434-4>
- Lana X, Rodríguez-Solà R, Martínez MD, Casas-Castillo MC, Serra C, Kirchner R (2020) Multifractal structure of the monthly rainfall regime in Catalonia (NE Spain): evaluation of the non-linear structural complexity. *Chaos* 30(7):3117. <https://doi.org/10.1063/5.0010342>
- Lana X, Rodríguez-Solà R, Martínez MD, Casas-Castillo MC, Serra C, Burgueño A (2020b) Characterization of standardized heavy rainfall profiles for Barcelona city: clustering, rain amounts and intensity peaks. *Theoret Appl Climatol* 142:255–268. <https://doi.org/10.1007/s00704-020-03315-z>
- Lana X, Rodríguez-Solà R, Martínez MD, Casas-Castillo MC, Serra C, Kirchner R (2021) Autoregressive process of monthly rainfall amounts in Catalonia (NE Spain) and improvements on predictability of length and intensity of drought episodes. *Int J Climatol* 41:3178–3194. <https://doi.org/10.1002/joc.4915>
- Liuzzo L, Freni G (2015) Analysis of extreme rainfall trends in Sicily for the evaluation of depth-duration-frequency curves in climate change scenarios *Journal of Hydrological Engineering*, 20(12). [https://doi.org/10.1061/\(ASCE\)HE.1943-5584.0001230](https://doi.org/10.1061/(ASCE)HE.1943-5584.0001230)
- Llabrés-Brustenga A, Rius A, Rodríguez-Solà R, Casas-Castillo MC, Redaño A (2019) Quality control process of the daily rainfall series available in Catalonia from 1855 to the present. *Theoret Appl Climatol* 137(3–4):2715–2729. <https://doi.org/10.1007/s00704-019-02772-5>
- Llabrés-Brustenga A, Rius A, Rodríguez-Solà R, Casas-Castillo MC (2020) Influence of regional and seasonal rainfall patterns on the ratio between fixed and unrestricted measured intervals of rainfall amounts. *Theoret Appl Climatol* 140:389–399. <https://doi.org/10.1007/s00704-020-03091-w>
- Mansell MG (1997) The effect of climate change on rainfall trends and flooding risk in the West of Scotland. *Hydrol Res* 28(1):37–50. <https://doi.org/10.2166/nh.1997.0003>
- Martínez MD, Lana X, Burgueño A, Serra C (2007) Spatial and temporal daily rainfall regime in Catalonia (NE Spain) derived from four precipitation indices, years 1950–2000. *Int J Climatol* 27:123–138. <https://doi.org/10.1002/joc.1369>
- Mc Night TL, Hess D, “Climate Zone and Types”, *Physical Geography. A Landscape appreciation*. Upper Saddle River, NJ, Prentice Hall, pp 200 (2000).
- Meinshausen M, Vogel E, Nauels A, Lorbacher K, Meinshausen N, Etheridge DM, Fraser PJ, Montzka SA, Rayner PJ, Trudinger CM, Krummel PB, Beyerle U, Canadell JG, Daniel JS, Enting IJ, Law RM, Lunder CR, O’Doherty S, Prinn RG, Reimann S, Rubino M, Velders GJM, Vollmer MK, Wang RHJ, Weiss R (2017) Historical greenhouse gas concentrations for climate modelling (CMIP6). *Geosci Model Dev* 10:2057–2116. <https://doi.org/10.5194/gmd-10-2057-2017>
- Menabde M, Seed A, Pegram G (1999) A simple scaling model for extreme rainfall. *Water Resour Res* 35(1):335–339. <https://doi.org/10.1029/1998WR900012>
- Miranda JD, Armas C, Padilla FM, Pugnaire FI (2011) Climatic change and rainfall patterns: effects on semi-arid plant communities of the Iberian Southeast. *J Arid Environ* 75:1302–1309. <https://doi.org/10.1016/j.jaridenv.2011.04.022>
- Mirhosseini G, Srivastava P, Stefanova L (2013) The impact of climate change on rainfall Intensity–Duration–Frequency (IDF) curves in Alabama, USA. *Reg Environ Chang* 13:25–33. <https://doi.org/10.1007/s10113-012-0375-5>
- Pérez FF, Boscolo R (2010) Clima en España: Pasado, presente y futuro. Informe de Evaluación del Cambio climático Regional. Red Temática CLIVAR-España. http://clivar.iim.csic.es/files/informe_clivar_final.pdf.
- Pérez-Zanón N, Casas-Castillo MC, Peña JC, Aran M, Rodríguez-Solà R, Redaño A, Sole G (2018) Analysis of synoptic patterns in relationship with severe rainfall events in the Ebre Observatory (Catalonia). *Acta Geophys* 66:405–414. <https://doi.org/10.1007/s11600-018-0126-1>
- Press WH, Teukolsky SA, Vetterling WT, Flannery BP (2007) *Interpolation by Kriging: Section 3.7.4. Numerical Recipes: the Art of Scientific Computing*, 3rd edition. New York: Cambridge University Press. ISBN:978–0–521–88068–8.
- Rodríguez R, Navarro X, Casas MC, Ribalaygua J, Russo B, Pouget L, Redaño A (2014) Influence of climate change on IDF curves for the metropolitan area of Barcelona (Spain). *Int J Climatol* 34:643–654. <https://doi.org/10.1002/joc.3712>
- Rodríguez-Solà R, Casas-Castillo MC, Navarro X, Redaño A (2017) A study of the scaling properties of rainfall in Spain and its appropriateness to generate intensity-duration-frequency curves from daily records. *Int J Climatol* 37(2):770–780. <https://doi.org/10.1002/joc.4738>
- Schertzer D, Lovejoy S (1987) Physical modelling and analysis of rain and clouds by anisotropic scaling multiplicative processes. *J Geophys Res* 92(D8):9693–9714. <https://doi.org/10.1029/JD092iD08p09693>

- Serra C, Fernández Mills G, Periago MC, Lana X (1998) Surface synoptic circulation and daily precipitation patterns in Catalonia. *Theor Appl Climatol* 59(1–2):29–49. <https://doi.org/10.1007/s007040050011>
- Sigró J, Brunet M, Aguilar E, Saladie O, López D (2005) Spatial and temporal patterns of Northeastern Spain temperature change and their relationships with atmospheric and SST modes of variability over the period 1950–1998. *Geophys Res Abstr* 7(04118):1–2 (EGU05-A-04118)
- Sneyers R (1990) On the statistical analysis of series of observation. Technical Note 415, World meteorological Office, WMO, Geneva, 192 pp.
- Stein ML (1999) *Statistical Interpolation of Spatial Data: some Theory for Kriging*. Springer, New York
- Stern DI, Kaufmann RK (2000) Detecting a global warming signal in hemispheric temperature series: a structural time series analysis. *Clim Change* 47:411–438. <https://doi.org/10.1023/A:1005672231474>

Publisher's note Springer Nature remains neutral with regard to jurisdictional claims in published maps and institutional affiliations.